Int. J. Electrochem. Sci., 15 **(2020)** 52 – 67, doi: 10.20964/2020.01.21

International Journal of
ELECTROCHEMICAL
SCIENCE
www.electrochemsci.org

Short Communication

High removal efficiency of dye pollutants by anodic Fenton treatment

V. Rondán[1], *B. Ramírez*[1], *S. Silva-Martínez*[2], *J.A. Hernández*[2], *Manoj Kumar Tiwari3,*
A. Alvarez-Gallegos[2,*]

[1] Posgrado en Ingeniería y Ciencias Aplicadas FCQeI-CIICAp, UAEM, Morelos.
[2] Centro de Investigación en Ingeniería y Ciencias Aplicadas. UAEM, Av. Universidad 1001, Cuernavaca Morelos, 62209. México. Tel/Fax: (777) 329 7084 and 329 777984.
[3] School of Water Resources, Indian Institute of Technology Kharagpur, Kharagpur – 721302, INDIA
[*]E-mail: aalvarez@uaem.mx

Received: 4 August 2019 / *Accepted:* 12 October 2019 / *Published:* 30 November 2019

Anodic Fenton treatment (AFT) has been extensively applied for water remediation. In general, three different bench-scale divided (salt bridge or ion membrane) reactors have been focused to treat small volumes (90-350 mL) and low concentration (20-400 μM) of organic pollutants in short treatment periods (2-40 min). The best experimental condition of AFT was found by performing several trails with different H_2O_2 concentrations continuously added. In this work a modified AFT reactor is proposed: a divided electrochemical flow cell (7.58×10^{-3} m s^{-1}) separating the catholyte from the anolyte by a treated cation permeable membrane. This electrochemical process has been focused to treat 2L of aqueous solutions of 1 mM acid orange 7 (AO7), 0.5 mM methylene blue (MB), and 0.12 mM reactive black 5 (RB5). The stoichiometric amount of H_2O_2 required was added in a single dose at the beginning of the electrolysis. At 40 min of electrolysis, a near complete discoloration of all dye solutions and COD reductions of 85%, 84% and 76% for AO7, MB and RB5 were obtained, respectively. Additionally, an industrial textile effluent (300 ppm COD) was successfully oxidized in 40 minutes of electrolysis, lowering 95% of the initial COD using the proposed AFT reactor. The energy requirements were low for the treatment of all the synthetic dye solutions ($\leq$0.041 kW h m^{-3}) and for the oxidation of the industrial wastewater (0.075 kW h m^{-3}). Furthermore, the AFT electrochemical reactor allows an economic cogeneration of H_2 (19.85 kW h kg^{-1} H_2) together with the treatment of textile effluents.

Keywords: Anodic Fenton treatment; Azo dyes; Catalytic H_2O_2 activation; H_2 production; Textile industry wastewater

1. INTRODUCTION

Anodic Fenton treatment (AFT) was first documented 20 years ago [1]. The chemistry behind AFT is the generation of highly reactive free radicals (probably a mixture of $OH^{\bullet}/HO_2^{\bullet}$) through a catalytic process carried out in a divided electrochemical reactor. This configuration allows a better control of the chemistry of the catholyte and anolyte. At the anolyte side, Fe^{2+} ions can be electrogenerated from a sacrificial iron or stainless steel (SS) anode (Eq. 1), while H_2O_2 is externally added to the anolyte.

$$Fe - 2e^- \rightarrow Fe^{2+} \qquad (1)$$

The advantage of this approach is that the H_2O_2 is activated by Fe^{2+} cations and the strong oxidant ($OH^\bullet/HO_2^\bullet$) is formed in the anolyte. Although the existence of hydroxyl radical is not settled satisfactorily [2, 3] it is accepted that the main $OH^\bullet$ production from the chemical interaction between H_2O_2 and Fe^{2+} could be described by Eq. 2 [4]:

$$Fe^{2+} + H_2O_2 \rightarrow Fe(OH)^{2+} + OH^\bullet \qquad (2)$$

Such free radicals are effective in destroying organic matter because they are reactive electrophiles that react rapidly with almost all electron-rich chemical compounds without any specific selectivity. The oxidation power of such radicals offers a great potential for water remediation.

In the catholyte side, H_2 is produced from H_2O reduction on a carbon cathode surface (Eq. 3):

$$2H_2O + 2e^- \rightarrow H_2 + 2OH^- \qquad (3)$$

The AFT approach was extensively applied on bench scale reactors for pesticide and herbicide abatement. The first AFT experiments were carried out in a pair of half-cells connected by a salt-bridge [1, 5]. Thereafter, the two half-cells were connected by either cationic [6, 7] or anionic [8-17] exchange membrane. Under the same approach, an H-type divided (anionic membrane) flow cell was also tested [12, 14, 16]. In general, the anode and cathode were made of iron plate (20-30 cm^2) and carbon, respectively. In all cases, the electrolysis current was controlled at 0.01-0.10 A to vary the Fe^{2+} delivery rate, while H_2O_2 was delivered at different volumetric velocities to maintain a desired $[Fe^{2+}]/[H_2O_2]$ ratio in the anolyte. AFT was focused to small volumes (90-350 mL) and low concentrations (20 - 400 μM) of pesticides/herbicides. For a given organic pollutant concentration in the anolyte, the best experimental condition of AFT was found by performing several trails with different $[Fe^{2+}]/[H_2O_2]$ ratios. Short treatment periods (2-40 min) were obtained to completely remove the parent compound and some of their primary byproducts. The oxidation of the target organic pollutant followed a first (or second) order kinetics degradation during the AFT. Therefore, the rate constant of the reaction is used to assess the treatment efficiency. One of the latest published works on AFT was proposed for an azo dye oxidation at low energy consumption. In this respect, the AFT was coupled to a microbial fuel cell (MFC). Each electrochemical system consisted of two half-cells separated by a cationic membrane. The energy required for the AFT was taken from the MFC [18]. Main results showed that under these conditions the 85% of 400 mL of 2 mM AO7 was oxidized in the MFC assisted-AFT process with 2 mM H_2O_2 in 20 min. The complete chemical oxidation of AO7 involves $102e^-$ reaction; however, color is expected to be removed at an early stage of oxidation. In all the aforementioned AFT works, this approach was efficient in eliminating the parent compound. However, a moot point of this approach is that the efficiency of the AFT can be evaluated in another way, such as considering the H_2O_2 consumed during organic oxidation. In other words, the fraction of the organic conversion (or the fraction of the H_2O_2 consumed) also provides a measure of AFT efficiency.

From the literature search (Scopus), after 2012 there are no more reports published and focused to the AFT. The objective of this study is to analyze the performance of a modified AFT reactor and its application to economically treat several synthetic solutions of azo-dye, including an industrial textile effluent. The originality of this proposed approach entails the following features: a) the divided electrochemical reactor is a potentially scalable flow cell, b) the reactor separator (treated cation membrane) allows a low energy consummation during the wastewater treatment, c) there is no need to perform several trails with different $[Fe^{2+}]/[H_2O_2]$ ratios to find out the best experimental conditions. The stoichiometric amount of H_2O_2 required was added in a single dose at the beginning of the electrolysis, d) the AFT allows an economic cogeneration of H_2.

2. EXPERIMENTAL

2.1 Solutions and Chemicals.

All chemicals were of reagent grade quality obtained from Sigma-Aldrich or JT Baker. Different concentrations of H_2O_2 were prepared from a 30% commercial H_2O_2 using distilled water. The rest of the aqueous solutions were prepared using laboratory tap water with the chemical composition indicated in Table 1. The synthetic dye solutions were prepared using industrial dyes such as acid orange 7 (AO7), methylene blue (MB) and reactive black 5 (RB5), supplied by Ciba Specialty Chemicals, and their properties are presented in Table 1.

Table 1. Main experimental conditions

Chemical composition of the tap water.

Ion	Na^+	Mg^{2+}	Ca^{2+}	K^+	Cu^{2+}	Fe^{2+}	Cl^-	SO_4^{2-}	PO_4^{3-}	Total Alkalinity as $CaCO_3$
ppm	130	5.5	3.2	2.6	<0.02	0.013	188	2.16	<0.001	65
pH	7.5									

Required energy to oxidize the dyes by means of electro Fenton/like-Fenton developed in the electrochemical reactor divided by a treated membrane. 2.0 L of anolyte containing dye + 0.05 M Na_2SO_4, pH 2. Applied potential 0.40 V; N/A = not available, MW = molecular weight, WW = industrial wastewater sample. 76 -95 % COD abatement.

Dye	mM	Condensed Formula	MW	λ max (nm)	Cell current (mA)	Initial COD (ppm)	mM H_2O_2 added	Energy (kW h m^{-3})
AO7	1.0	$C_{16}H_{11}NaO_4S$	350.3	483	310	520	40.8	0.041
RB5	0.12	$C_{26}H_{21}Na_4N_5O_9S_6$	999.8	597	300	130	10.8	0.040
MB	0.50	$C_{16}H_{18}ClN_3S$	373.9	661	210	215	23.4	0.028
WW	N/A	N/A	N/A	515	565	300	80	0.075

An industrial wastewater sample from a dying bath effluent (cloudy blue color, high quantity of solids in suspension, pH 12, COD = 5500 mg L^{-1}, and 1915 mS cm^{-1}) was provided by a Mexican textile industry (Zacatepec, Morelos State) for the degradation in the modified AFT electrochemical reactor.

2.2. Electrodes and Cell.

The electrochemical cell was a parallel plate reactor divided by a Nafion® 117 membrane as described elsewhere [22], as depicted in Fig. 1. It was made of four blocks of acrylic and the inner blocks were machined to form the compartments of the catholyte and analyte, each of almost 700 mL. Both electrodes were made of mesh (0.20 m × 0.21 m, with 7 threads per cm) of commercial carbon steel. Four gaskets (made of sheets of silicon rubber) were set between blocks and the membrane to avoid leaks.

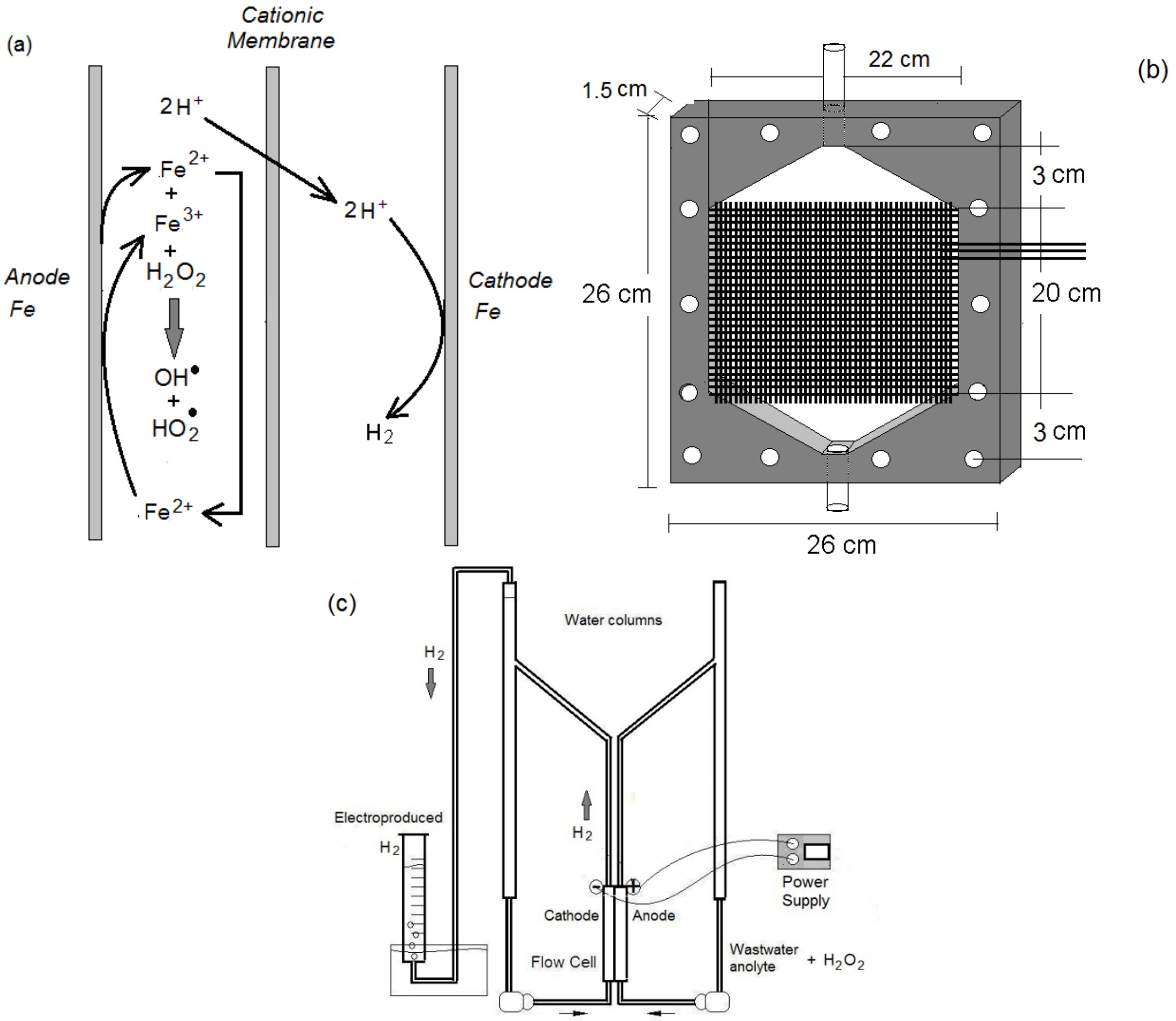

Figure 1. (a) Schematic representation of the electrochemical reactions expected in the reactor; (b) Catholyte compartment and Fe-cathode (0.20 m × 0.21 m); (c) Hydraulic circuit (4 L in total) and flow cell.

A schematic representation of the electrochemical reactions expected in the reactor are shown in Fig. 1a. The geometry of the catholyte compartment with the Fe-cathode is shown in Fig. 1b (without endplate). The Fe-anode and its endplate were identical in the anolyte compartment. To improve the evacuation of the H_2 produced from the Fe-cathode, catholyte and anolyte compartments were pressurized with 0.60 m water columns and both electrolytes were continuously pumped (1.5 L min^{-1}, 0.00758 m s^{-1} on the electrodes surfaces) through the electrochemical reactor. The hydraulic circuit (4 L) and the flow cell are depicted on Fig. 1c.

2.3. Membrane Treatment.

The Nafion® 117 membrane was boiled to increase its conductivity in the following three solutions [23]: (1) 3% H_2O_2 for 1 h, (2) 0.5 M H_2SO_4 for 3 h and (3) deionized water for 3 h. After this procedure, the membrane was activated and ready to be used.

2.4. Measurements.

The electrochemical experiments were controlled using a BK precision power d. c. supply (model 1786 DC). The electrical charge was integrated from tabular data (current *vs*. time) taken manually from the power supply display. The quantitative analysis of H_2O_2 was carried out following the procedure of the permanganate method [24]. The absorbance was measured as a function of the wavelength using a Hach spectrophotometer DR/4000 UV-Vis. The H_2 was collected under water in a graduated cylinder at room temperature (25°C) and atmospheric pressure (1 atm). The number of H_2 moles was estimated based on the volume of H_2 electrogenerated using the ideal gas law. The H_2 production was always a linear function of the charge (*e.g.* [H_2] = slope x charge) under the conditions studied. For each experiment the experimental slope (*ES*) was evaluated by the linear least square method. The current efficiency (ϕ) of the hydrogen production is linked to the theoretical slope (*TE*) according to Eq.4.

$$\phi(\%) = (ES/TE) \cdot 100 \qquad (4)$$

TE was calculated using the law of Faraday:

$$m = (1/nF)\, q \qquad (5)$$

Where m is the amount (in moles) of H_2 produced, n is the number of electrons, F is the Faraday constant (96 485 A s mol^{-1}) and q is the electrical charge (A s). The energy efficiency (Φ) of the cell was evaluated with the Eq.6.

$$\Phi(\%) = E(_{HHV}/E_{Cell}) \cdot 100 \qquad (6)$$

Where E_{HHV} = 1.481 V, the higher heating-value voltage [25]. The energy consumption (E, in $kWhm^{-3}$) for wastewater treatment can be calculated from Eq.7, taking into account the electrolysis time

($t_{Electrolysis}$, in h), assuming an average cell current (I_{Cell}, in A), cell voltage (E_{Cell} , in V) and the volume of catholyte ($V_{Anolyte}$, in m^3).

$$E = (E_{Cell})(I_{Cell})(t_{Electrolysis})/V_{Anolyte} \qquad (7)$$

The COD was estimated as an indicator of the amount of organic matter in the samples. The COD was analyzed by a HACH® procedure using standard reagents and standard method that involves the digestion of the aqueous sample followed by the spectrophotometric determination of COD (DR/4000 UV-Vis).

3. RESULTS AND DISCUSSION

3.1 Required H_2O_2.

Although the interactions of the soluble iron cations with H_2O_2 produce a strong oxidant (which identity is still controversial), the chemistry behind the Fenton related process is one of the most difficult set of chemical/electrochemical reactions. Therefore, the predictions of the main chemical/electrochemical reactions are a challenging task [19- 21]. However, in a simplified mechanism the catalytic activation of H_2O_2 (each mole gains 2e$^-$) can be described by the following reaction:

$$H_2O_2 + 2H^+ + 2e^- \rightarrow 2H_2O \qquad (8)$$

The Eq. 8 should be the basis to evaluate the AFT efficiency. The AFT was carried out in a divided electrochemical flow cell where the catholyte and anolyte were separated by a cation permeable membrane. In the anolyte two main tasks were performed: a) the catalytic activation of H_2O_2 and b) the degradation of several synthetic azo dyes effluents (containing AO7, MB and RB5) and an industrial textile effluent. While in the catholyte (pH 0), an effective electroproduction of H_2 was carried out.

Catalytic activation of H_2O_2 (pH 2) was performed in the absence of organic pollutant, a desirable quantity of H_2O_2 was added in a single dose before the start of electrolysis. As soon as the electrolysis begins, the iron anode spontaneously produces Fe^{2+}, Eq. 9

$$Fe - 2e^- \rightarrow Fe^{2+} \qquad (9)$$

However, at a sufficiently positive anode potential Fe^{2+} can be oxidized to Fe^{3+}, according to Eq. 10:

$$Fe^{2+} - e^- \rightarrow Fe^{3+} \qquad (10)$$

H_2O_2 is catalytically activated by the interactions of soluble iron cations (Fe^{2+}/Fe^{3+}). Following a complex Fenton chemistry, a mixture of strong oxidants (probably a mixture of $OH^\bullet$/$HO_2^\bullet$) is generated. From a practical point of view, the H_2O_2 activation (Fenton and Fenton-like reaction) can be simplified to represent the near-stoichiometric generation of a strong oxidant from de available H_2O_2, Eq. 8.

Therefore, the sum of the electrochemical reactions of the proposed AFT, such as the conventional cathodic generation of H_2 and the proposed anodic generation of Fe^{3+}, gives the following global reaction:

$$2H^+ + 2Fe^{2+} \rightarrow H_2 + 2Fe^{3+} \qquad (11)$$

Fig. 1a shows a schematic representation of the expected electrochemistry in the AFT electrochemical system using a cathode and an anode made of iron. The required energy for driving the reaction (11) is 148.4 kJ mol^{-1}. Thus, it is 88.7 kJ mol^{-1} less than the energy consumed in a conventional PEM electrolyzer.

Under this approach, a desirable quantity of an organic compound in the anolyte can be degraded by the stoichiometric H_2O_2 activated. This fact allows estimating both: the kinetics and the theoretical assessment of the oxidation of dye compounds. The complete theoretical oxidation of AO7 is a 68-electron oxidation reaction, Eq. 12:

$$C_{16}H_{11}O_4N_2SNa + 32H_2O - 68e^- \rightarrow 16CO_2 + 68H^+ + NaHSO_4 + 2NH_3 \qquad (12)$$

Considering the latter suppositions, the stoichiometric oxidation of AO7 by catalyzed H_2O_2 in the anolyte is given by Eq. 13:

$$C_{16}H_{11}O_4N_2SNa + 34H_2O_2 \rightarrow 16CO_2 + NaHSO_4 + 2NH_3 + 36H_2O \qquad (13)$$

Following the same suppositions as above, the theoretical oxidation of MB and RB5 are represented by Eq. 14 and Eq. 15, respectively:

$$C_{16}H_{18}N_3SCl + 39H_2O_2 \rightarrow 16CO_2 + H_2SO_4 + 3NH_3 + HCl + 42H_2O \qquad (14)$$

$$C_{26}H_{21}O_{19}N_5Na_4S_6 + 76H_2O_2 \rightarrow 26CO_2 + 4H_2SO_4 + 5HNO_3 + 2Na_2SO_4 + 80H_2O \qquad (15)$$

3.2 H_2O_2 Catalytic Activation.

The catalytic activation of H_2O_2 by the electrogenerated iron ions was indirectly studied in the electrochemical reactor at room temperature using a flow rate (catholyte and anolyte) of 7.58x10^{-3} m s^{-1}. The anolyte and the catholyte consisted of 0.05M Na_2SO_4 (pH 2 fixed with H_2SO_4) and 1 M H_2SO_4, respectively. The amount of the strong oxidants produced by the H_2O_2 activation was evaluated indirectly by measuring the concentration difference between the initial and the remaining H_2O_2 in solution ([$\triangle H_2O_2$]). The H_2O_2 activation rate (AR) was computed as [$\triangle H_2O_2$]/t. The performance of the untreated cation membrane at 1.0 V (1.0 A) and the chemically treated cation membrane at 0.4 V (0.57 A) for the H_2O_2 AR at different H_2O_2 concentrations is reported in Fig. 2 and 3, respectively (symbols represent experimental data).

In both cases, almost 90% of the initial H_2O_2 was activated at quasi constant rate (2 mM min^{-1}) following a pseudo zero-order kinetic degradation, represented by a continuous line. The dashed lines represent the actual H_2O_2 catalytic activation. There was no apparent effect of the H_2O_2 initial concentration on its AR. Although the H_2O_2 AR was not significantly different for the chemically treated and untreated cation membrane, the energy required for H_2O_2 activation increases as a function of the initial H_2O_2 concentration. The energy required to activate 70 mM H_2O_2 (2L) using the treated cation membrane was approximately 60% lower (1.6 W h mol^{-1} H_2O_2) compared to 4.1 Wh mol^{-1} H_2O_2, when using the untreated cation membrane in 35 min of electrolysis.

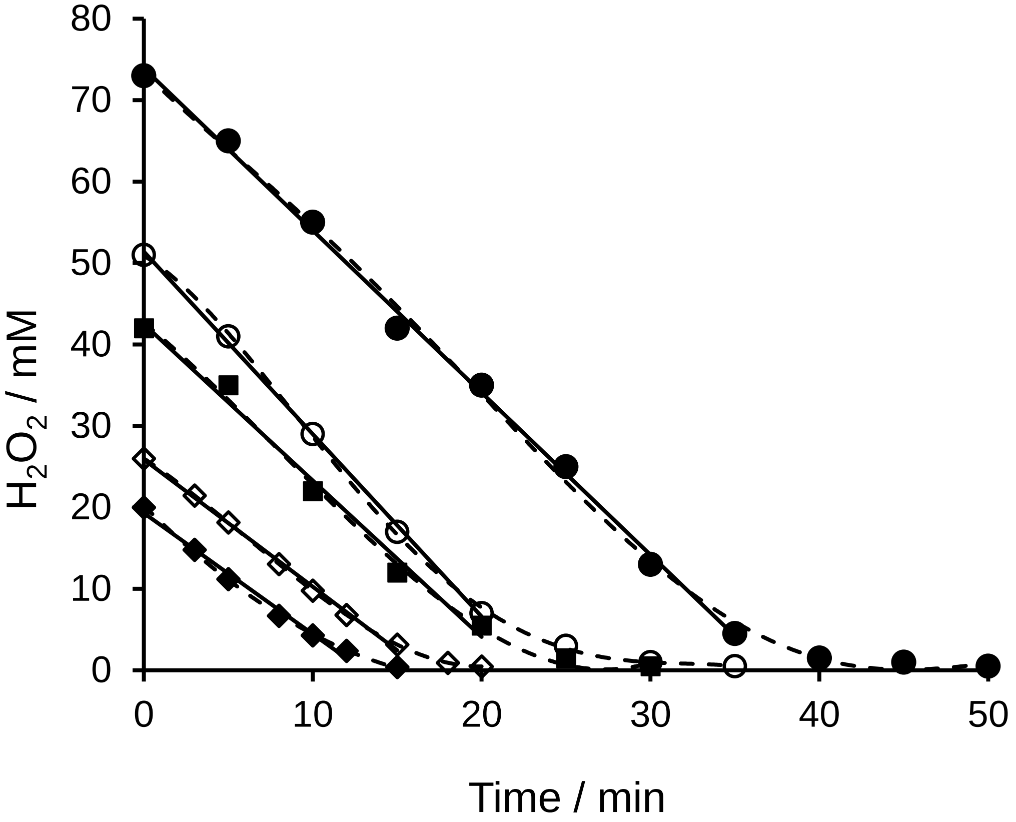

Figure 2. AR of H_2O_2 for 73 mM (●), 51 mM (○), 42 mM (■), 26 mM (□) and 20 mM (♦) of H_2O_2 in the reactor working with an untreated membrane at 1.0 V (1.0 A). The solid line represents a pseudo zero-order kinetic with constant rate (2 mM min^{-1}), while dashed line represents the actual H_2O_2 catalytic activation.

3.3. Oxidation of Synthetic Azo Dyes.

The oxidation of the synthetic azo dyes AO7, MB and RB5 (Table 1) was investigated individually in the anolyte compartment of the electrochemical reactor at room temperature using a flow rate (catholyte and anolyte) of 7.58×10^{-3} m s^{-1}. The degradation studies were conducted for 40 min treating 2 L of aqueous solutions of 1.0 mM AO7, 0.5 mM MB, and 0.12 mM RB5. The main experimental conditions are described in Table 1. According to the Eq. 13 the complete oxidation of 1.0 mM AO7 (with an initial COD = 520 ppm) requires 34 mM H_2O_2. Similarly, the theoretical H_2O_2 requirement for complete oxidation of 0.5 mM of MB and 0.12 mM RB5 was estimated using equations (14) and (15) as 19.5 mM and 9.12 mM of H_2O_2, respectively.

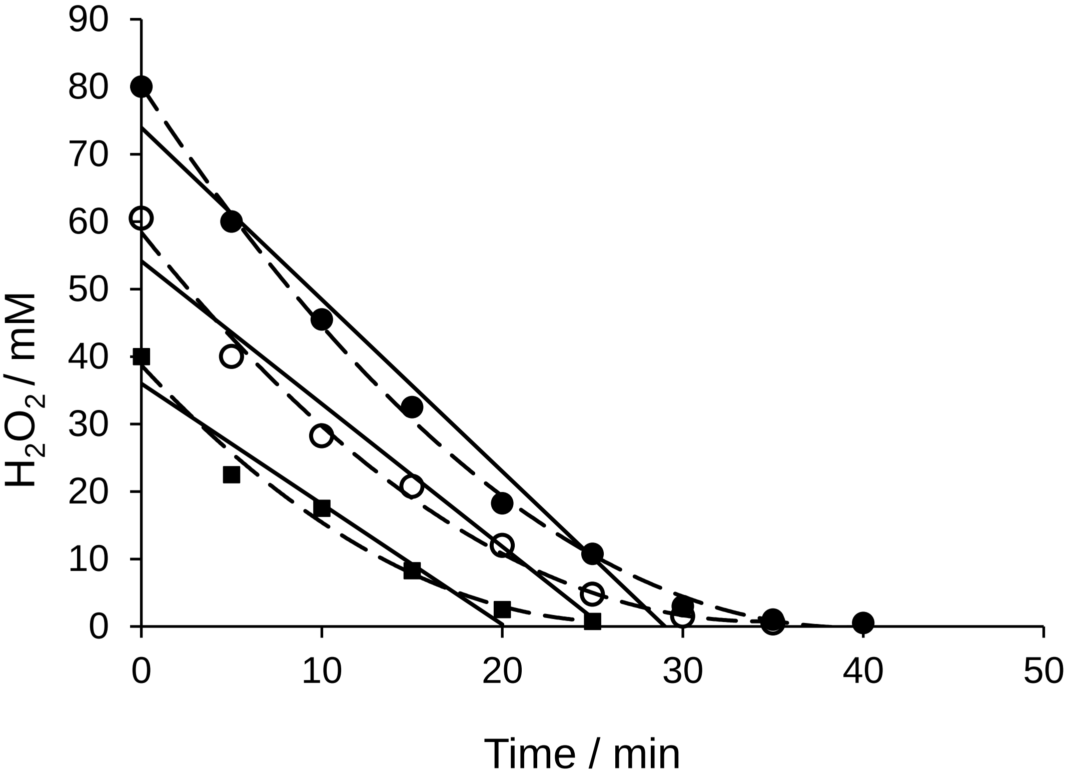

Figure 3. AR of H_2O_2 for 80 mM (●), 60 mM (○) and 40 mM (■) of H_2O_2 in the reactor working with a treated membrane at 0.4 V (0.57 A). The solid lines represent a pseudo zero-order kinetic with constant rate of 2 mM min^{-1}, while dashed lines represent the actual H_2O_2 catalytic activation.

However, in the present study the oxidations were carried out using a 20% excess of the required concentration of H_2O_2 for each azo dye to compensate for transfer limitations. Therefore, the oxidations of AO7, MB and RB5 were carried out in the presence of 40.8 mM, 23.4 mM, and 10.8 mM of H_2O_2, respectively.

The spectra of the initial dye solutions were recorded before treatment (diluting 100 times each test solution) and at the end of the electrolysis (40 min) without any dilution. These spectra are shown in Fig. 4, 5 and 6 for AO7 (COD 520 ppm), MB (COD 215 ppm), and RB5 (COD 130 ppm), respectively.

At 40 min of electrolysis, COD reductions of 85%, 84%, and 76% were recorded for AO7, MB, and RB5, respectively. All the dye samples exhibited near complete discoloration. The COD removal efficiencies were better or comparable to the earlier reported values for each of AO7 [26, 27, 28], MB [29, 30, 31], and RB5 [32, 33] for such a short electrolysis time.

The energy consumption for the removal of AO7 at 0.40 V (0.310 A) was estimated (Eq. 7) as 0.041 kW h m^{-3}. Similarly, removal of MB, at 0.40 V (0.210 A), and RB5, at 0.40 V (0.300 A), required 0.028 kW h m^{-3} and 0.04 kW h m^{-3} energy consumptions, respectively. The low energy consumption in the process is attributed to the modified cation membrane that improves the overall performance of the AFT electrochemical reactor.

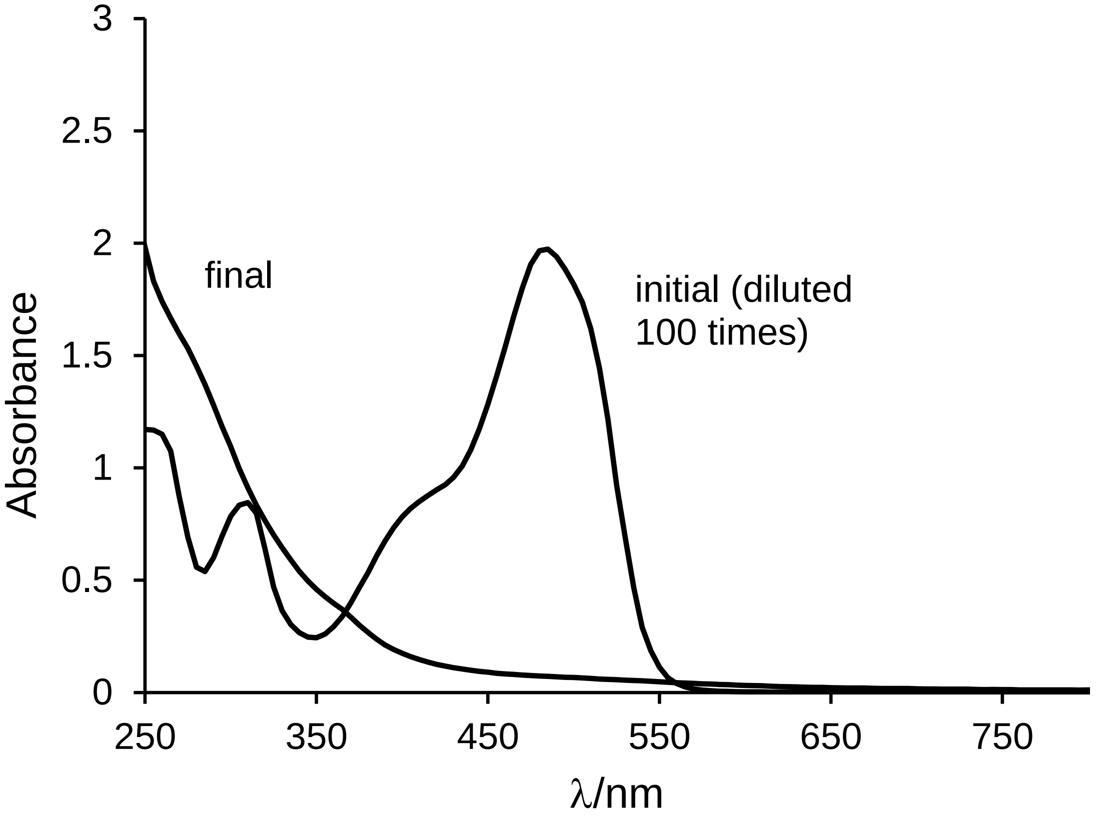

Figure 4. Initial absorbance spectrum recorded from a synthetic industrial effluent containing 1 mM AO7 (COD = 520 ppm) + 0.05 M Na_2SO_4 (pH 2) (abs 1.97 at λ_{max} = 483 nm). Final absorbance spectrum recorded (without dilution) from a treated solution initially containing 1 mM AO7 + 40.8 mM H_2O_2 (COD = 520 ppm) + 0.05 M Na_2SO_4 (pH 2) + a treated membrane at 0.4 V (0.310 A) (abs 0.074) at 40 min of electrolysis (COD = 78 ppm).

3.4. Treatment of the Industrial Effluent.

The raw effluent from the dying bath (with a large amount of total suspended solids, pH 12, and COD 5500 ppm) was first pretreated through filtration and its pH was adjusted to 2 to prevent the precipitation of $Fe(OH)_3$. After this physical treatment, the COD dropped to 1600 ppm. A series of 2 L volume of the diluted wastewater (0.05 M Na_2SO_4, COD = 300 ppm) were systematically oxidized at 0.40 V (0.565 A) for 40 min using different concentrations of H_2O_2 in the AFT electrochemical reactor. The spectra of the samples post electrolysis at initial concentrations of H_2O_2 equal to 22, 44, 61 and 80 mM are shown in Fig. 7a along with a control sample in the absence of H_2O_2. It is evident that the degree of color removal increased with increasing H_2O_2 levels.

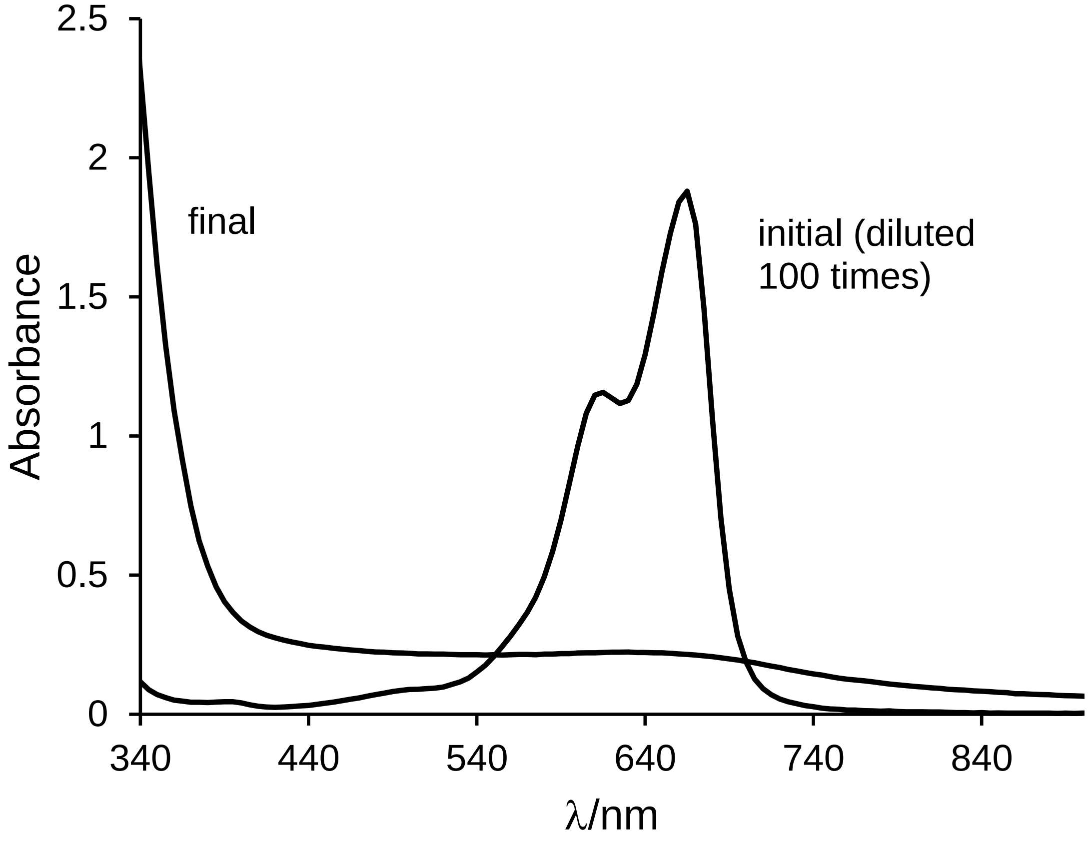

Figure 5. Initial absorbance spectrum recorded from a synthetic industrial effluent containing 0.5 mM MB (COD = 130 ppm) + 0.05 M Na_2SO_4 (pH 2) (abs 1.88 at λ_{max} = 661 nm). Final absorbance spectrum recorded (without dilution) from a treated solution initially containing 0.5 mM MB + 23.4 mM H_2O_2 (COD = 130 ppm) + 0.05 M Na_2SO_4 (pH 2) + a treated membrane at 0.4 V (0.210 A) (abs 0.219) at 40 min of electrolysis (COD = 34 ppm).

The final COD values, at 40 min of electrolysis, were recorded as 147, 50, 34 and 14 ppm with 22, 44, 61 and 80 mM H_2O_2, respectively. The levels of COD were reduced exponentially (Fig. 7b) with P-value of 0.0003 that indicates a statistically highly significant correlation. As a result, the COD removal can be modeled as:

$$\ln(C/C_0) = -m[H_2O_2] \qquad (16)$$

The slope (m) of the linear regression of a plot of the concentration of H_2O_2 (mM) *vs*. ln(C/C_0), from Eq.16, was calculated as 0.038±0.002 mM^{-1}; where C_0 and C are the initial (300 ppm) and final

COD concentrations recorded at the end of the electrolysis for different H_2O_2 concentrations. The energy requirement for the 95% COD removal for this industrial diluted textile effluent was estimated as 0.075 kW h m^{-3}. This energy requirement is much lower compared with those reported earlier [34].

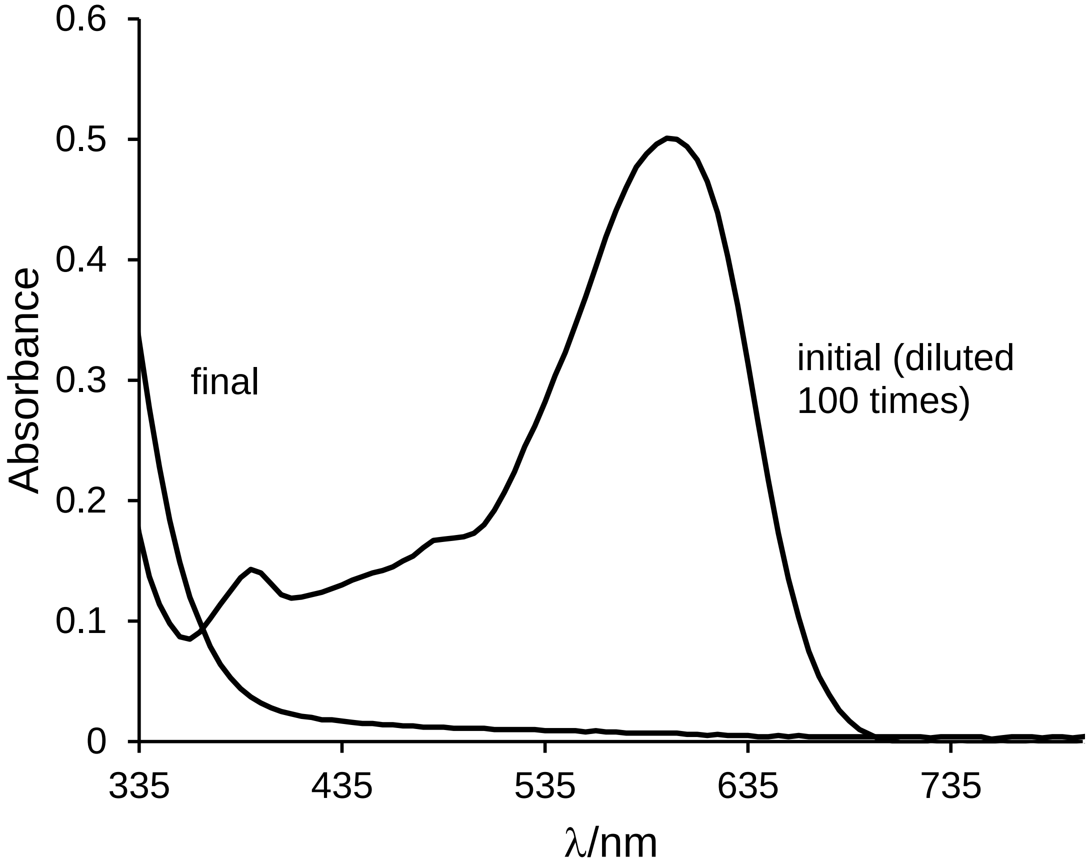

Figure 6. Initial absorbance spectrum recorded from a synthetic industrial effluent containing 0.12 mM RB5 (COD = 215 ppm) + 0.05 M Na_2SO_4 (pH 2) (abs 0.501 at λ_{max} = 597 nm). Final absorbance spectrum recorded (without dilution) from a treated solution initially containing 0.12 mM RB5 + 10.08 mM H_2O_2 (COD = 215 ppm) + 0.05 M Na_2SO_4 (pH 2) + a treated membrane at 0.4 V (0.300 A) (abs 0.007) at 40 min of electrolysis (COD = 35 ppm).

Along with the electrolysis of the organic pollutants in the anolyte, the AFT simultaneously produced H_2 by reducing H^+ at the carbon steel cathode. The production of H_2 was estimated during the oxidation of the textile wastewaters. The H_2 was electro produced as a linear function of the charge passed in the catholyte compartment of the electrochemical reactor, operating at 0.40V (0.58A).

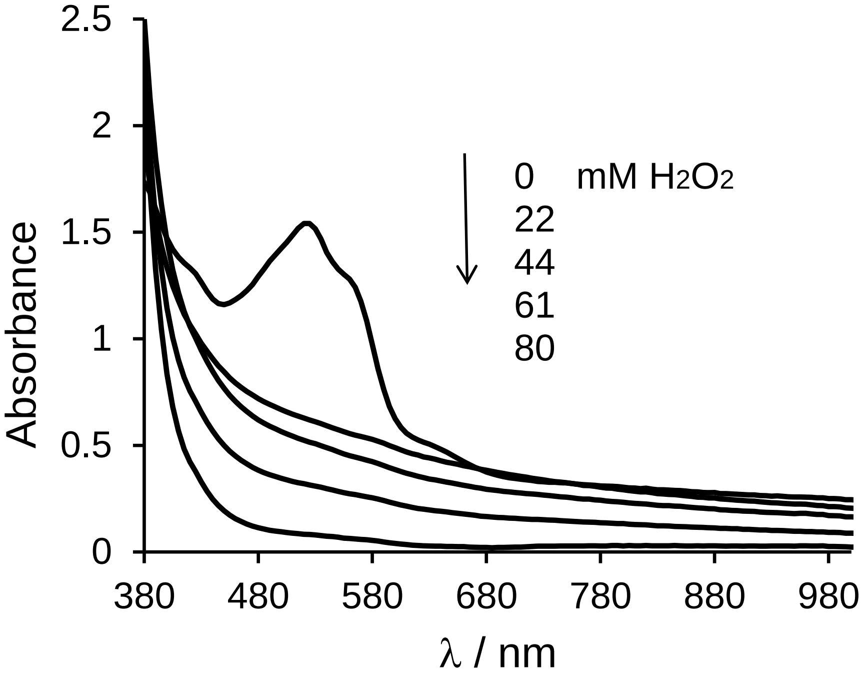

(a)

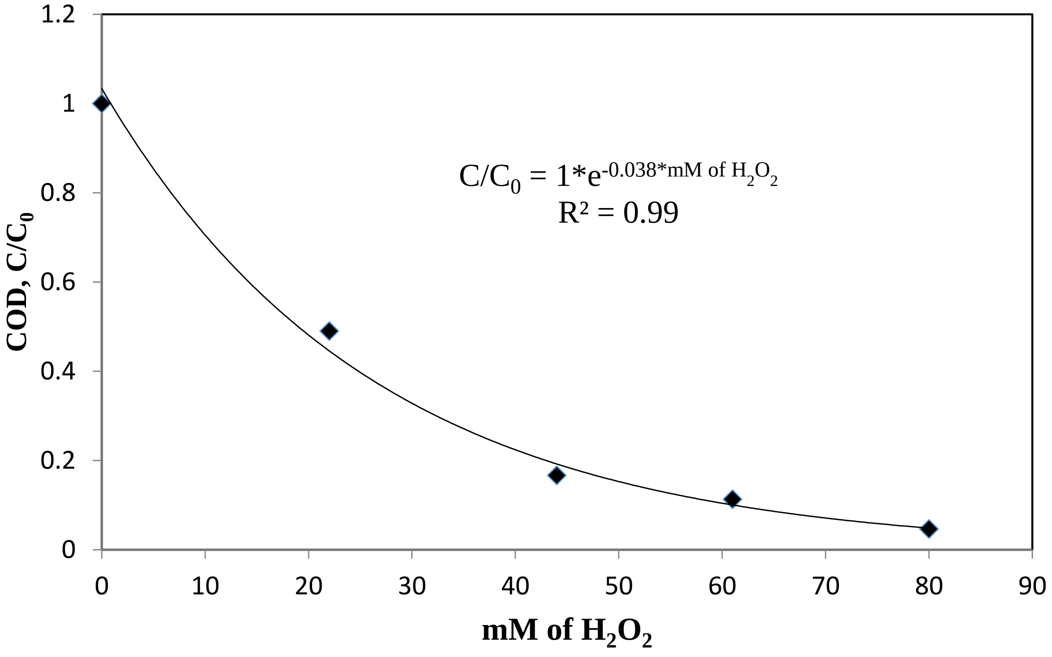

(b)

Figure 7. (a) Absorbance spectra of the untreated diluted industrial effluent and electrolyzed (40 min each) industrial effluent with a treated membrane at 0.4 V (0.565 A) with different H_2O_2 concentrations. From top to bottom: the first spectrum represents the initial diluted textile wastewater without electrochemical treatment, the second, third, fourth and fifth correspond to 22, 44, 61 and 80 mM H_2O_2, respectively; (b) COD removal *vs.* H_2O_2 concentrations for the industrial effluent electrolyzed for 40 min with a treated membrane at 0.4 V and 0.565 A. C/C_0 refers to the ratio of the final COD after electrolysis to the initial COD of the diluted wastewater (300 ppm).

A production of H_2 of 0.192 L was collected in a graduated cylinder with water during the electrolysis that lasted 40 min. This volume became moles of H_2 considering the ideal gas equation. From the plot of moles of H_2 *vs.* charge (not shown) and the law of Faraday (Eq. 4 and 5), the current efficiency for H_2 production was evaluated as 97%. Using the Eq. 6, the energy efficiency (Φ) was 370%. This is possible, because the Fe^{3+}electrogeneration (Eq. 2) is a more efficient energy reaction than the O_2 evolution reaction. In other words, the H_2 production was using just the 27% of the E_{HHV} value. The energy requirements for H_2 production are 0.812 W h L^{-1} (19.85 kW h kg^{-1} H_2). This value is well below the energy requirements (53.4-70.1 kW h kg^{-1} H_2) of a typical commercial electrolyzer system [35]. The AFT system investigated here provides high oxidation efficiencies (considering the reduction of COD and the fraction of H_2O_2 consumed) of non-biodegradable azo dyes with low energy requirement along with the production of H_2 as a profitable by-product.

4. CONCLUSIONS

A modified electrochemical reactor is proposed and used for the AFT of azo dyes. For this purpose, the catalytic activation of H_2O_2 was carried out with a chemically treated cation membrane and an untreated cation membrane. With an untreated cation membrane, 90% of a wide range of H_2O_2 concentrations (from 20 to 80 mM) was rapidly activated at room temperature (with a near constant H_2O_2 AR of 2 mM min^{-1}) by the electrogenerated iron ions at 1.0 V (1.0 A). However, under the same experimental conditions the same H_2O_2 AR (generating a strong oxidant) is obtained. But, in this case, the applied energy was reduced 40% when the chemically treated cation membrane was used.

The present study demonstrates that AFT can be applied economically to treat synthetic effluents from azo dyes when the stoichiometric amount of H_2O_2 required is added in a single dose at the beginning of the electrolysis. The three azo dyes tested (2 L of aqueous solutions of 1 mM AO7, 0.5 mM MB, and 0.12 mM RB5) showed near complete discoloration and COD reductions of 85, 84 and 76 %, respectively, at 40 min of electrolysis. The industrial textile effluent, prefiltered and diluted to decrease the initial COD concentration to 300 ppm, was oxidized resulting in a 95% COD removal. The energy requirements were low for the treatment of all synthetic dye solutions ($\leq$0.041 kW h m^{-3}) and for the oxidation of industrial wastewater (0.075 kW h m^{-3}). Furthermore, the AFT electrochemical reactor allows an economic cogeneration of H_2 (19.85 kW h kg^{-1} H_2) together with the treatment of textile effluents.

ACKNOWLEDGMENTS
The authors gratefully acknowledge the financial support of both Mexican SEP-PROMEP and FORDECYT (CONACyT) programs.

DECLARATION OF INTEREST
The authors do not have conflicts of interest in the publication of this manuscript.

References

1. A. Saltmiras, A.T. Lemley, *J. Agric. Food Chem.,* 48 (2000) 6149-6157. https://doi.org/10.1021/jf000084v
2. J.F. Perez-Benito, *J. Phys. Chem. A.,* 108 (2004) 4853-4858. doi: 10.1021/jp031339l.
3. B. Ensing, F. Buda and E.J. Baerends, *J. Phys. Chem.,* A., 107 (2003) 5722-5731. doi: 10.1021/jp0267149 EJ
4. B. Boye, E. Brillas and M. Dieng, *J. Electroanal. Chem.,* 540 (2003) 25–34. https://doi.org/10.1016/S0022-0728(02)01271-8
5. Q. Wang, A.T. Lemely, *Environ. Sci. Technol.,* 35 (2001) 4509-4514. doi.org/10.1021/es0109693
6. Q. Wang, A.T. Lemley, *J. Agric. Food Chem.,* 50 (2002) 2331-2337. https://doi.org/10.1021/jf011434w.
7. E. M. Scherer, Q.-Q. Wang, A.G. Hay, A.T. Lemley, *Arch. Environ. Contam. Toxicol.,* 47 (2004) 154-161. doi: 10.1007/s00244-004-3102-5
8. Q. Wang, A.T. Lemley, *J. Agric. Food Chem.,* 51 (2003) 5382-5390. https://doi.org/10.1021/jf034311f.
9. Q. Wang, E.M. Scherer, A.T. Lemley, *Environ Sci. Technol.,* 38 (2004) 1221-1227 https://doi.org/10.1021/es0345827
10. L. Kong, A.T. Lemley, *J. Agric. Food Chem.,* 54 (2006) 3941-3950. https://doi.org/10.1021/jf060046x
11. C.L. Friedman, A.T. Lemley, A. Hay, *J. Agric. Food Chem.,* 54 (2006) 2640-2651. doi.org/10.1021/jf0523317
12. L. Kong, A.T. Lemley, *J. Agric. Food Chem.,* 54 (2006) 10061-10069. https://doi.org/10.1021/jf062110g.
13. K. Neafsey, X. Zeng, A.T. Lemley, *J. Agric. Food Chem.,* 58 (2010) 1068–1076. doi:10.1021/jf904066a
14. H. Zhang, A.T. Lemley, Environ. Sci. Technol., 40 (2006) 4488-4494. doi: 10.1021/es060515b
15. L. Kong, A. T. Lemley, *Water Res.,* 41 (2007) 2794-2802. doi:10.1016/j.watres.2007.03.001
16. H. Zhang, A.T. Lemley, *J. Agric. Food Chem.,* 55 (2007) 4073-4079. https://doi.org/10.1021/jf070104u.
17. X. Xiao, X. Zeng, A.T. Lemley, *J. Agric. Food Chem.,* 58 (2010) 10169-10175. doi:10.1021/jf101943c
18. X-W. Liu, X-F. Sun, D-B. Li, W-W. Li, Y-X. Huang, G-P. Sheng, H-Q. Yu, *Water Res.,* 46 (2012) 4371-4378. doi:10.1016/j.watres.2012.05.044
19. F, Buda, B. Ensing, M.C.M. Gribnau, E.J. Baerends, *Chem Eur J.,* 7 (2001) 2775-2783
20. B. Ensing, F. Buda, P. Blöchl, E.J. Baerends, *Angew Chem Int Ed.,* 40 (2001) 2893-2895. doi:10.1002/1521-3773(20010803)40:15<2893::AID-ANIE2893>3.0.CO;2-B
21. S. Rachmilovich-Calis, A. Masarwa, N. Meyerstein, D. Meyerstein, R. van Eldik, *Chem Eur J.*, 15 (2009) 8303-8309. doi:10.1002/chem.200802572
22. I. Navarro-Solís, L. Villalba-Almendra, A. Alvarez-Gallegos, *Int. J. Hydrogen Energ.,* 35 (2010) 10833-10841**.** https://doi.org/10.1016/j.ijhydene.2010.07.086
23. L. Napoli, J. Franco, H. Fasoli, A. Sanguinetti, *Int. J. Hydrogen Energ.,* 39 (2014) 8656-8660. https://doi.org/10.1016/j.ijhydene.2013.12.066
24. I.M. Kolthoff, R. Belcher, Volumetric Analysis. Vol III. Interscience Publishers, Inc (1957) New York. USA
25. R.L. LeRoy, Ch.T. Bowen, D.J. LeRoy, *J. Electrochem. Soc.,* 127 (1980) 1954-1962. doi: 10.1149/1.2130044
26. O. Scialdone, A. Galia, S. Sabatino, *Electrochem Commun.,* 26 (2013) 45-47. https://doi.org/10.1016/j.elecom.2012.10.006
27. V. Elias, E. Vaschetto, K. Sapag, M. Oliva, S. Casuscelli, G. Eimer, *Catal Today.,* 172 (2011) 58–

65. https://doi.org/10.1016/j.cattod.2011.05.003
28. A. Wang, W. Guo, F. Hao, X. Yue, Y. Leng, *Ultrason Sonochem.,* 21 (2014) 572–575. https://doi.org/10.1016/j.ultsonch.2013.10.015
29. N. Shimizu, C. Ogino, M.F. Dadjour, T. Murata, *Ultrason Sonochem.,* 14 (2007) 184-190. doi:10.1016/j.ultsonch.2006.04.002.
30. A. Sandoval-González, S. Silva-Martínez, *Ultrason Sonochem.,* 15 (2008) 1038-1042. https://doi.org/10.1016/j.ultsonch.2008.03.008.
31. L. Jiménez-Lima, S. Silva-Martínez, J.A. Hernández, F.Z. Sierra, A. Alvarez-Gallegos, *Desalin Water Treat.,* 55 (2015) 3646-3652. doi:10.1080/19443994.2014.939864.
32. M.S. Lucas, J.A. Peres, *Dyes Pigments.,* 71 (2006) 236-244. https://doi.org/10.1016/j.dyepig.2005.07.007
33. X. Liu, M. Qiu, Ch. Huang, *Procedia Engineering.,* 15 (2011) 4835-4840. doi:10.1016/j.proeng.2011.08.902
34. S. Figueroa, L. Vázquez, A. Alvarez-Gallegos, *Water Res.,* 43 (2009) 283-294. https//doi.org/10.1016/j.watres.2008.10.014
35. J. Turner, G. Sverdrup, M.K. Mann, P.Ch. Maness, B. Kroposki, M. Ghirardi, R.J. Evans, D. Blake, *Int. J. Energ Res.,* 32 (2008) 379-407. https://doi.org/10.1002/er.1372